Proc. Schl. Eng. Tokai Univ., Ser. E
41 (2016) 31-37

Structural Characteristics of New Composite Girder Bridge Using Rolled Steel H-Section

by

Mohammad Hamid ELMY[*1] and Shunichi NAKAMURA[*2]

(Received on Mar. 30, 2016 and accepted on May 12, 2016)

Abstract

Bridges using rolled steel H-section seem very economical compared with welded plate girder bridges due to lower material and fabrication cost. On the other hand, as the maximum web height is 900 mm, the applicable span length of the girder bridge with rolled H-section is up to 20 m or 25 m. A new composite girder bridge was proposed using rolled steel H-section. The superstructure is a continuous girder with rolled steel H-section and RC slab, and the substructure is an RC pier. The girder and the pier are rigidly connected by concrete and reinforcements. This new SRC bridge is basically a multi-span rigid frame structure: the steel/concrete composite girder resists at the span center, and the steel girder covered by RC section resists at the rigid joints. The proposed SRC bridge allows the span length to be increased up to 50 m, and is much cheaper to construct than the conventional plate girder bridge.

Keywords: Composite girder bridge, Rolled steel H-beam, Compact section, Limit states design, Experimental investigation, Non-linear analysis

1. Introduction

The bridge using rolled steel H-section is expected to be economical compared with the welded plate girder bridges due to lower material and fabrication cost for short span bridges. Besides, the rolled steel H-section is a compact section and has favorable bending characteristics and no need for stiffeners. However, as the maximum available web height of the rolled H-sections is 900mm, the applicable span length for simple span is up to 20m and for continuous spans up to 25m.

A new composite girder bridge was proposed using rolled steel H-section[1)] (Fig.1). The super-structure is a continuous girder with rolled steel H-section and the RC slab, and the substructure is RC piers. The girder and the pier are rigidly connected by concrete and reinforcements. The proposed SRC girder with the rolled H-section could extend the applicable span length up to 50m. When the bridge has a continuous form, the area around the intermediate supports is always more critical than that of span center. Hence the rolled H-beams are strengthened around the intermediate supports by covering the joint with reinforced concrete, which forms SRC and increase the bending capacity.

A rolled H-girder has high ultimate strength with good ductile property, attains full plastic moment and is regarded as the compact section. The deflection of the SRC Bridge due to the design live load is expected to be small and satisfy the serviceability limit state. The super-structure is rigidly connected to the pier and seems to have better performance against earthquakes. A trial design and experiments were conducted in this study, showing that the proposed SRC bridge using rolled H-section is feasible and economical.

2. Trial Design

2.1 *Bridge model*

A trail design was carried out for a two lane four-span continuous girder highway bridge with the span length of 40+50+50+40 m, consisting of five girders of steel rolled H-section with a web height of 900mm, as shown in Fig.2 and Fig.3. The concrete piers are 10m high and 3.0m wide, and are rigidly connected to girders. The steel /concrete composite girder is proposed for the sagging bending moment at the span center (Fig.4a) and the steel girder covered by

*1 Graduate Student, Course of Civil Engineering
*2 Professor, Department of Civil Engineering

reinforced concrete section is proposed for the hogging bending moment at the rigid joints near support (Fig.4b).

The thickness of the concrete slab and its effective flange width is specified as per design code. About 15% of the span length near support joints are being covered by reinforced concrete section. The SRC section is reinforced with maximum allowed rebar percentage. As for the material properties for trail design, steel with tensile strength of 490 MPa was used for H-girders, and yield strength of 390 and 490 MPa for rebar. For the RC slab and piers, concrete with a specified compressive strength of 40MPa was used. The two girders, G1 and G3, were taken as the representative girders of the proposed bridge.

.

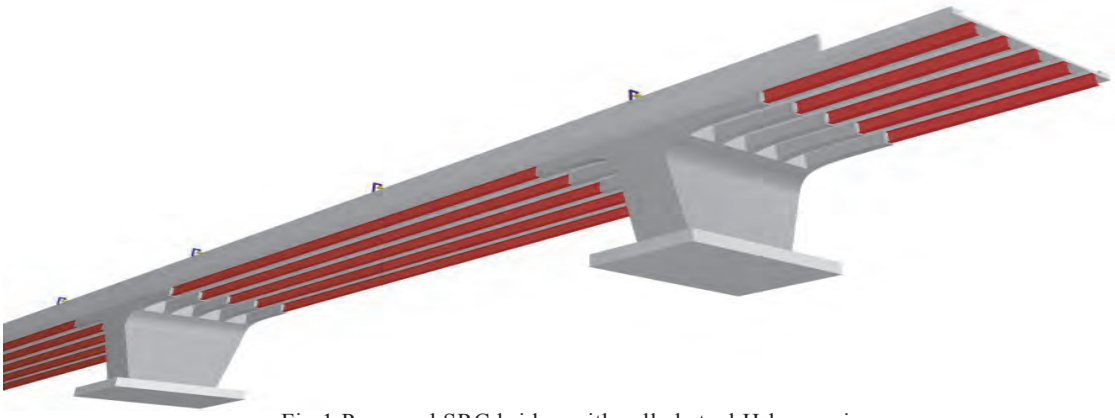

Fig.1 Proposed SRC bridge with rolled steel H-beam pipes

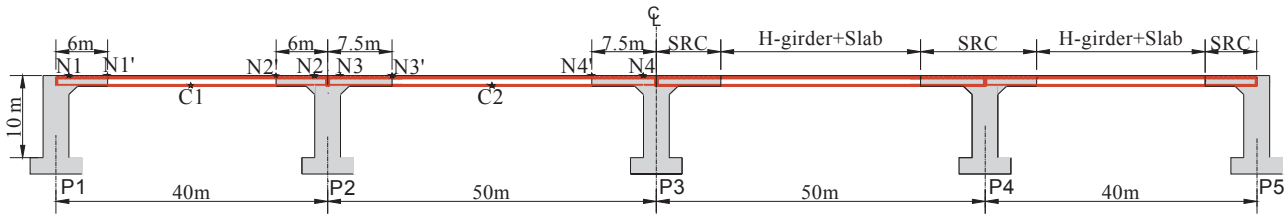

Fig.2 Side view of the model bridge

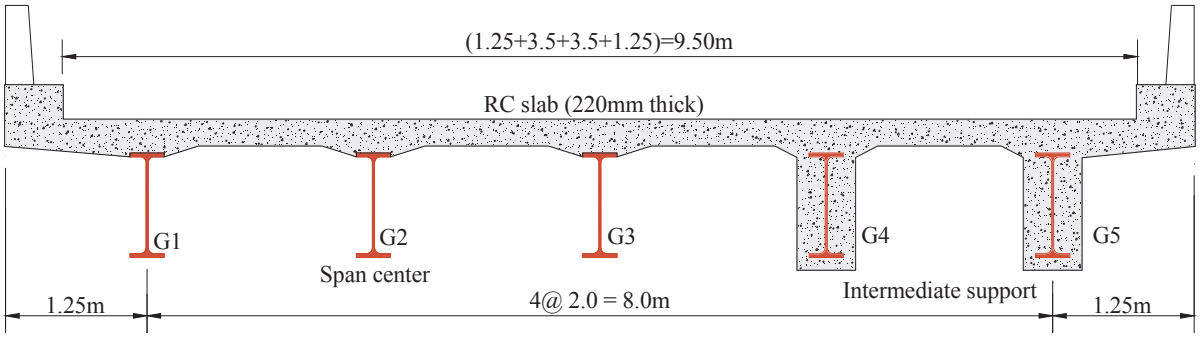

Fig.3 Cross-section of the model bridge

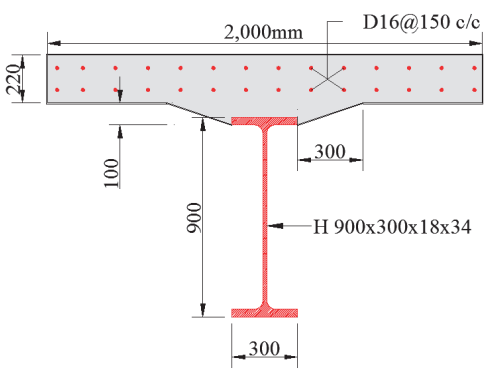

Fig.4a Section at span center

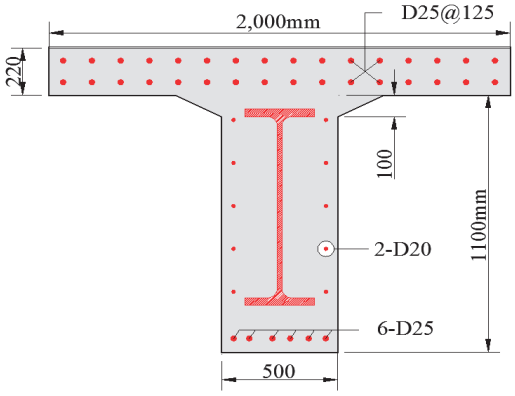

Fig.4b Section at intermediate support

2.2 ***Constitutive law of materials***

For structural computations, the stress-strain curve of concrete and steel was used to model the overall material behavior based on the JSCE code. The density of concrete was assumed to be 2400 kg/m^3 and the poison's ratio of concrete was taken as 0.2. The modulus of elasticity of concrete is defined as follows:

$$E_c = 8500(f'_{ck})^{\frac{1}{3}} \quad (1)$$

Where, f '$_{CK}$: is specified compressive strength of concrete (N/mm^2).

The non-linear elastic-plastic behavior of the concrete in compression including strain softening was represented by an equivalent uniaxial stress-strain curve, as shown in Fig.5. The model is expressed by the following equations:

$$\sigma'_c = E_0 K (\varepsilon'_c - \varepsilon'_p) \geq 0 \quad (2)$$

$$E_0 = \frac{2 . f'_{cd}}{\varepsilon'_{peak}} \quad (3)$$

$$K = exp\left\{-0.73 \frac{\varepsilon'_{max}}{\varepsilon'_{peak}} \left(1 - \exp\left(-1.25 \frac{\varepsilon'_{max}}{\varepsilon'_{peak}}\right)\right)\right\} \quad (4)$$

$$\varepsilon'_p = \varepsilon'_{max} - 2.86 . \varepsilon'_{peak} \left\{1 - \exp\left(-0.35 \frac{\varepsilon'_{max}}{\varepsilon'_{peak}}\right)\right\} \quad (5)$$

Where σ'$_c$: concrete stress, E$_0$: initial Young Modulus of concrete, ε'$_c$: concrete strain, ε'$_p$: plastic strain K: residual rate of elastic stiffness ε'$_{peak}$: peak strain corresponding to compressive strength (generally assumed 0.002), ε'$_{max}$: maximum strain, f'$_{cd}$: is design compressive strength of concrete (N/mm^2).

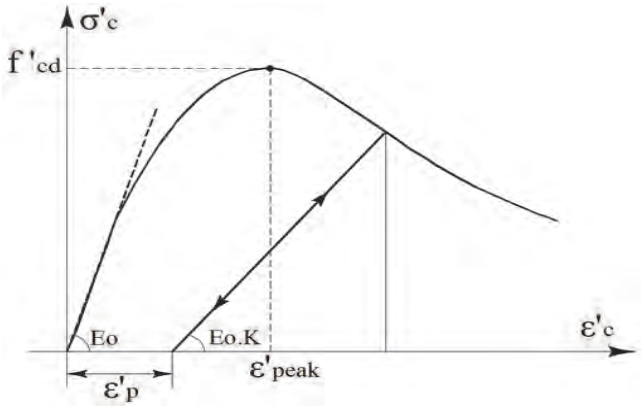

Fig.5 Stress-strain relationship of concrete in compression

For concrete in tension, as illustrated in Fig.6, the tensile stress was assumed to increase linearly with the strain until the concrete cracks. After the concrete cracks, the tensile strength decrease non-linearly with a tension stiffening effect. The tensile strength was given by following equations:

$$f_t = 0.23(f'_{cd})^{\frac{2}{3}} \quad (6)$$

$$\sigma_t = f_t \left(\frac{\varepsilon_{tu}}{\varepsilon_t}\right)^{0.4} \quad (7)$$

Where, f$_t$: design tensile strength of concrete (N/mm^2), ε$_t$: average of concrete tensile strain, ε$_{tu}$: cracking strain.

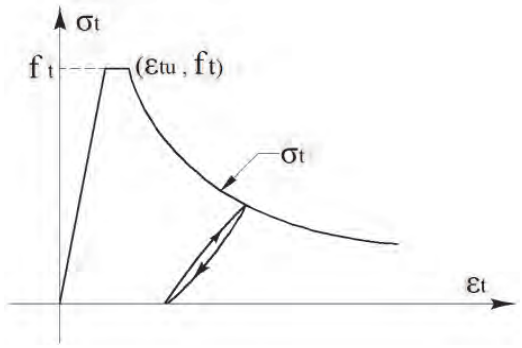

Fig.6 Stress-strain relationship of concrete in tension

The density of the steel in all of the components was assumed to be 7800 kg/m^3. A plastic model with von Mises' yield function associated plastic flow and isotropic hardening was used to model all steel parts. The modulus of elasticity and Poisson's ratio of steel were taken as 200 GPa and 0.3 respectively. The material behavior of the steel girder was represented by the tri-linear stress-strain relation shown in Fig.7. The yield strength f$_{sy}$, yield strain Ɛ$_{sy}$ and the ultimate strength f$_{su}$ need to be input to define the stress-strain curve, while the strain at the onset of strain hardening Ɛ$_{sh}$ and the ultimate strain limit Ɛsu were assumed to be 0.015 and 0.10, respectively. The true stress and strain values are given as input to the analysis model. For the steel reinforcement a simple elastic-perfectly plastic model without strain hardening behavior is employed.

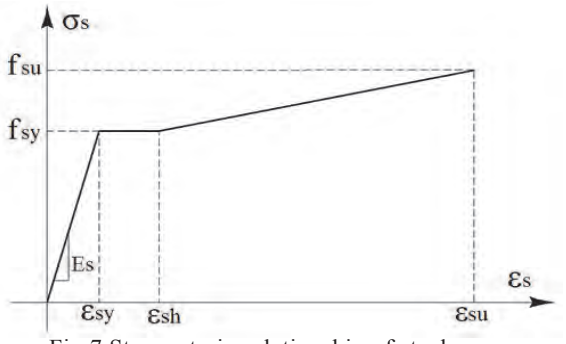

Fig.7 Stress-strain relationship of steel

2.3 ***Design loads***

The two kinds of design dead loads (D) of super-structure are considered: pre-composite dead load (D1) due to self-weight of girders, fresh concrete of the slab and form work, and the post-composite dead load (D2) due to the surface wearing, railings and traffic barriers.

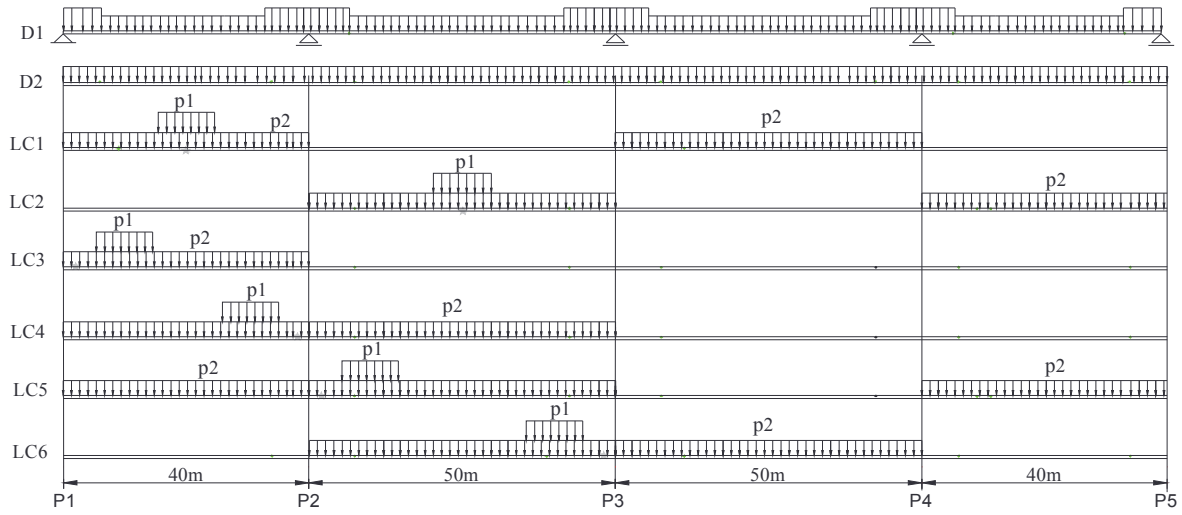

Fig.8 Design load cases

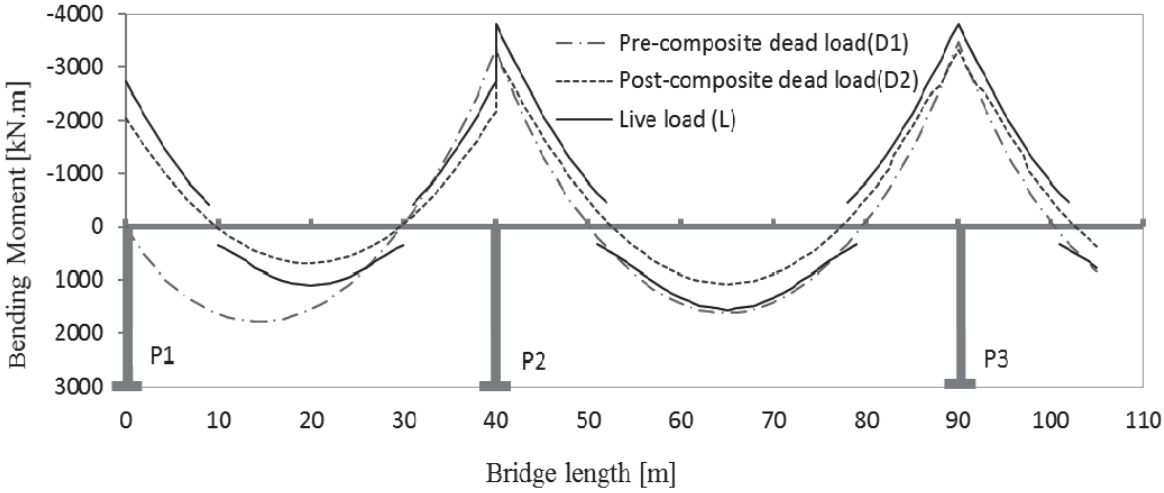

Fig.9 Design bending moment diagram

The design live load (L) and the impact effect (I) is adopted from Japanese highway bridge specification[2]. The B-live load consists of equivalent concentrated load (p1=10 kN/m^2) with the load length of 10m transversely and fully uniform distributed load of (p2=3.5 kN/m^2) with main lane width of 5.5m along the bridge. The live load impact factor is assumed as 20% based on the span length. Six live load cases, LC1 to LC6, were applied to the bridge model to obtain the maximum and the minimum sectional force and deformation at specified points, as shown in Fig.8.

2.4 ***Sectional forces***

The static analysis of full three dimensional model of the bridge with beam element was performed to obtain sectional forces and deformations. The analysis was conducted for pre-composite case with the continuous beam model, and for the post-composite and live load cases with the 3D rigid frame model.

The bending moment at span center and support joints are illustrated in Fig.9, which shows the bending moment diagram of the exterior girder (G1) due to pre-composite dead load (D1), post-composite dead load (D2) and live load (L) cases. The deflections due to live load cases are within the specified limit and satisfy the serviceability requirement.

2.5 ***Safety verification***

Safety verification was carried out by the limit states design method to ensure load carrying capacity of the composite girders throughout the service life of the structure against possible actions. Verification for prevention of member failure of the composite girder is conducted according to the following equation:

$$\gamma_i \frac{S_d}{R_d} \leq 0 \qquad (8)$$

Where, Sd: design sectional force, Rd: design sectional resistance capacity, and γi: structural factor. Load factors and material factors are determined in accordance with Guidelines for performance verification of steel–concrete hybrid structures[3]. The fiber model is used for flexure behavior of composite and SRC sections in order to obtain the bending moment-curvature (M-ϕ) relation. The cross section is divided into small fibers and each fiber conforms to the constitutive law of steel, concrete and reinforcing bar. The non-linear uniaxial stress-strain relation of these materials play a key role in the model.

Fig.10 and Fig.11 show the stress distribution of the sections for positive bending at span center and for negative bending near intermediate supports, respectively. The design bending moment (Md) was determined by the critical load combinations. The safety of each section is verified before and after formation of composite action in accordance with Guidelines for performance verification of steel–concrete hybrid structures[3]. To verify the sections before formation of composite action, the design bending moment due to pre-composite dead load (Md1) is taken only by the plastic bending capacity of the steel H-girder (Msud). To verify the sections after formation of composite action the design bending moment (Md) due to D1+D2+L is resisted by the ultimate bending resisting capacities (Mud) of the composite and SRC sections at the span center (positive B.M) and the joints (negative B.M), respectively. Table 1 and Table 2 are the verification results which show that the sections before and after formation of composite action at all anticipated points satisfied the criteria specified by the design specification. It was found that, the SRC section at support joint has around 1.7 times bending capacity than the composite section at span center.

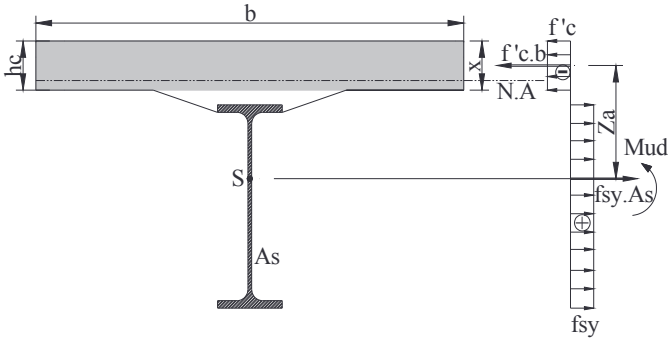

Fig .10 Stress distribution of span center

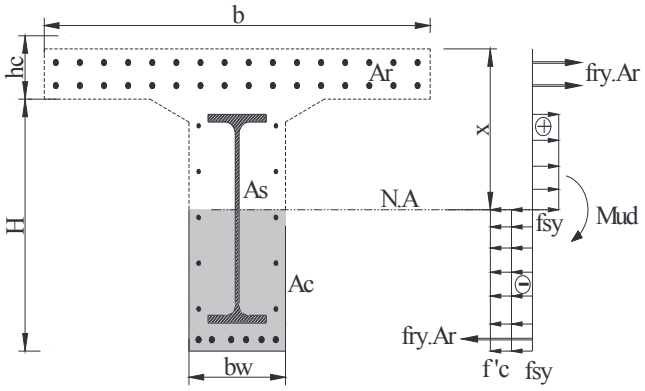

Fig .11 Stress distribution of support joint

Table 1 Verification of section before formation of composite action

Position	Design Bending Moment M_{d1} (kN.m)	Bending Moment Resisting Capacity M_{sud} (kN.m)	Safety check $(M_{d1}/M_{sud})*Y_i$	Verification
N1	0	3200	0.00	OK
C1	1950	3200	0.67	OK
N2	-2860	-3200	0.98	OK
N3	-2950	-4100	0.79	OK
C2	1780	4100	0.48	OK
N4	-3080	-4100	0.83	OK

Table 2 Verification of section after formation of composite action

Position	Design Bending Moment M_{d1} (kN.m)	Bending Moment Resisting Capacity M_{sud} (kN.m)	Safety check $(M_{d1}/M_{sud})*Y_i$	Verification
N1	-6430	-11400	0.62	OK
N1’	-2770	-5800	0.53	OK
C1	4710	6700	0.77	OK
N2	-9550	-13700	0.77	OK
N2’	-3710	-5800	0.70	OK
N3	-1278	-14700	0.96	OK
N3’	-4500	-6900	0.72	OK
C2	6140	7900	0.85	OK
N4	-12960	-14700	0.97	OK
N4’	-4530	-6900	0.72	OK

3. Experimental Investigation

3.1 *Test model and method*

A bending experiment was conducted with partial SRC model to investigate the bending strength and ductile characteristics of the steel-concrete rigid joint[4], as shown in Fig.12. The objective of this test was to clarify the load transfer mechanism from the girder to the pier at the rigid joint. The specimen was scaled down to half of the actual bridge, using the rolled H-section with 440mm high. The embedded length of girder was approximately twice the girder height.

The cross section of the pier is 1.0m by 0.9m. Perfo-bond rib (PBL) was used to perform sufficient bond and prevent shear slip between steel girder and concrete at the rigid joint. PBL were welded on the upper and lower flanges of the H girder. The number of holes in the PBL at the upper flange was more than that of the lower flange due to the difference of the shear stress.

Since it has become difficult to arrange the slab rebar in two layers similar to the actual bridge model, it was arranged in one layer at the slab center because of the slab thickness. The vertical stiffener is used at the loading point because of occurrence of stress concentration. The incremental load was applied and the vertical and horizontal displacements were recorded at each stage (e.g. cracking, yielding, and maximum) of any structure components. The geometrical dimension of the designed specimen is shown in Fig.13.

3.2 *Test result*

Fig.14 shows the relationship of applied load and vertical displacement of the test specimen at the loading position, and Fig.15 the horizontal displacement. The slab concrete cracks appeared at 80kN and the pier concrete started cracking at 131kN with the stiffness reduction. After that, the displacement continued to increase until the pier rebar yielded at 390kN.

Fig .12 Test set up photography

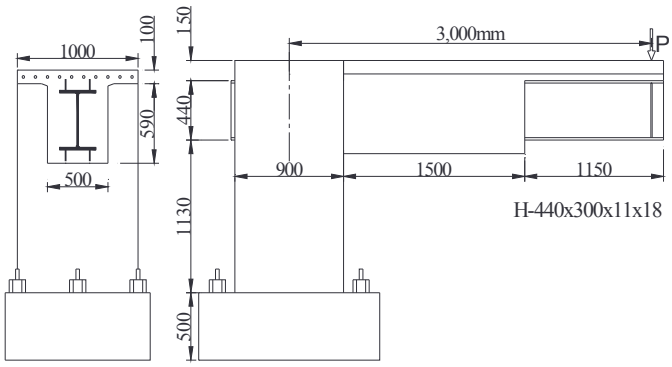

Fig .13 Dimension of test model

After yield of the pier rebar the rotation of pier increased and consequently both vertical and horizontal

displacement increased sharply. The load still increased and the test was terminated when the vertical displacement reached at about 100mm with the corresponding load of 625kN due to the limitation of the test equipment. At this load the concrete cracks occurred on the RC slab. These test results show that the proposed SRC section has sufficient bending strength and good ductility.

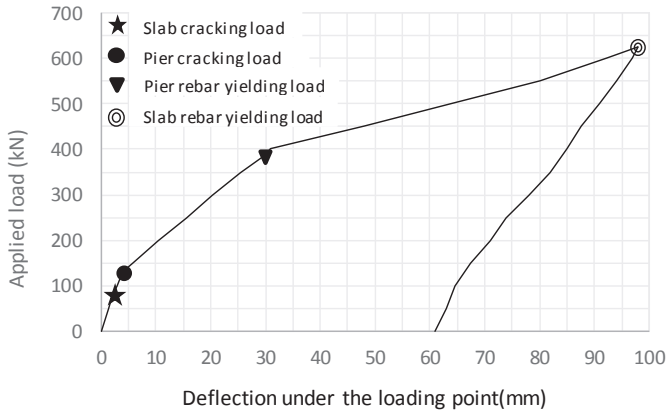

Fig .14 Load vs vertical displacement

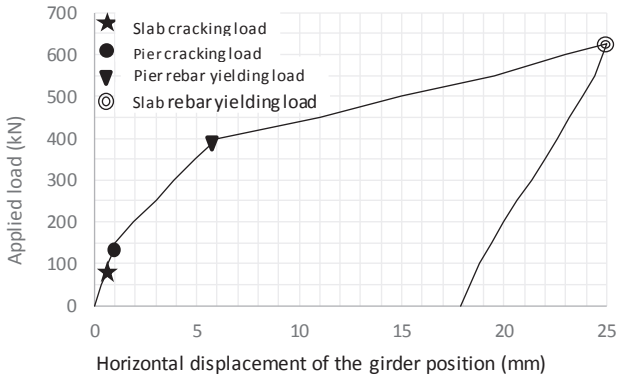

Fig .15 Load vs horizontal displacement

4. Numerical Analysis

Non-linear numerical analysis of the experimental model was performed in order to verify its consistency. The fiber model was used for all structural components, conforming to relevant material constitutive law and hysteresis.

The numerical and experimental results are compared in the load-deflection plot shown in Fig.16. The analytical results agreed well with experimental results. The bending stiffness curve changed when cracks of the RC pier occurred and the steel rebar yielded at the pier, and the maximum bending strength was the same. In particular, both numerical and experimental load-deflection curve agreed in the initial elastic region up to about 130 kN.

Although the general behavior is almost the same, there is some difference in curve up to a load value of 400 kN. There are many factors which affect the bending behavior such as concrete mechanical property in the pier, shear connector at the rigid joint, reinforcement pitch, mesh size and so on. Further study with FEM analysis is necessary.

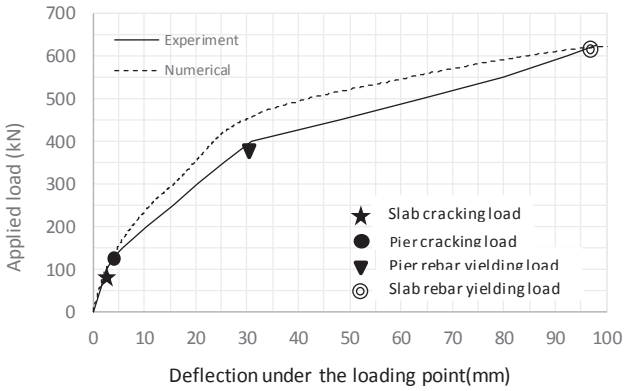

Fig .16 Comparison of load-deflection behavior

5. Conclusions

A new SRC bridge was proposed and a trial design was carried out, showing that the proposed SRC bridge with rolled steel H-section can extend the maximum span length up to 50.0 m. This is more than double the existing similar type of bridges. This new bridge is very economical compared with the conventional built-up (welded) girder bridge.

Bending tests were conducted with the rolled steel H-section covered with RC section and RC slab, showing that the proposed structural form had sufficient bending strength and concrete cracks were within the acceptable limit.

In conclusion, the proposed composite girder bridge using rolled steel H-section is feasible, economical and attractive.

References

1) Nakamura, S., Momiyama, Y., Hosaka, T. and Homma, K.: New technologies of steel/concrete composite bridges, Elsevier, Journal of Constructional Steel Research, Vol.58, pp.99-130, 2002.
2) Japan Road Association: Specifications for highway bridges, I. General, II. Steel Bridges, 2014
3) Japanese Association of Civil Engineers: Guidelines for performance verification of steel–concrete hybrid structures, 2006.
4) Takagi, M., Nakamura, S. and Muroi, S: An experimental investigation on rigid frame steel-concrete composite girder bridge, Journal of Structural Engineering, JSCE, Vol.49, No.32, 2003.